SNS 107080400-TD0001-R00

Chopper Design and Operation for the EQ-SANS

Jinkui Zhao

Spallation Neutron Source

Issued on: March 2003

1. Introduction

The Extended Q-Range Small Angle Scattering Instrument (EQ-SANS) [ref 1] (Fig. 1) on the 60Hz SNS target is designed to have high intensity, high precision, and large Q-coverage. The machine is located on beam line No. 6, facing the downstream, upper, coupled hydrogen moderator. The instrument is designed to have variable detector to moderator distances. Since the maximum usable neutron bandwidth is inversely proportional to the detector distance, the EQ-SANS requires a chopper system that allows variable neutron frame widths. In the initial design, the EQ-SANS has three double-disk bandwidth choppers. The openings of the choppers can be changed by the relative phases of the two disks. Double-disk choppers would offer the maximum operational flexibility for the EQ-SANS. The bandwidth choppers that are included in the SNS-project baseline are three single-disk choppers. Because the opening of these single-disk choppers cannot be varied once they are made and installed, careful design is needed for the opening angles of the choppers to maximize neutron fluxes on sample while minimizes leakages of neutrons into higher frames.

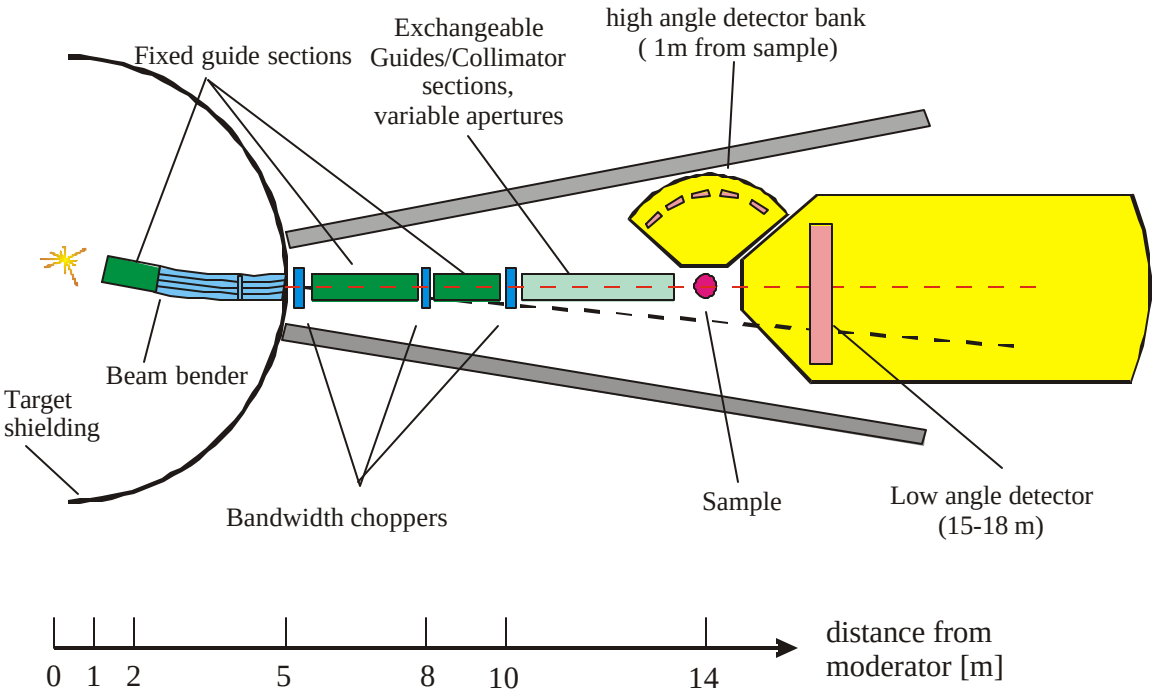

Figure 1. Conceptual sketch of the EQ-SANS, adapted from [1].

This document describes the design and operations of the bandwidth choppers on the EQ-SANS. In the first chapter, the methodology and various terms that are used for the design are briefly described. Chapter 2 summarizes the chopper design parameters in terms of the chopper locations, and for single disk choppers, the sizes of the chopper windows. Chapter 3 considers the usage of double-disk choppers at the chosen chopper location. The discussions in this chapter form the basis for further discussions. Chapter 4 tests the design of the single-disk choppers for various possible operational conditions on the EQ-SANS. Chapter 5 looks into the case of replacing one single-disk choppers with a double-disk one for future upgrade.

In all the studies in chapter 3-5, we tested chopper operations for leakages from longer wavelength and delayed neutrons. Since using three bandwidth choppers will not be sufficient to remove all neutron leakages at higher wavelength, we use 35Å as our wavelength criteria for these leakage tests. The chopper performances are considered acceptable if there are no undesired neutron leakages below 35Å. Neutrons with even longer wavelengths will be removed from the incident beam by a beam reflector. The beam reflector is described in the last Chapter 7.

1.1 Terminologies

Here is a list of terms that are used in this document.

Frame
A ***Time Frame*** is defined as the time interval between two consecutive source pulses. The wavelength band that corresponds to a *time frame* is the ***Wavelength Frame***. Both the time and wavelength frames are sometimes simply referred to as the ***Frame***. The width of a *time frame* is referred to as the frame's ***Time Width***. The width of the wavelength frame is referred to as the frame's ***Wavelength Width*** (see Figure 3).

The ***first frame*** is the time between the initial pulse and the following pulse. However, because the EQ-SANS is not designed to use neutrons with wavelength below 1Å, the ***first frame*** referred to in this document starts from 1Å, instead of the theoretical 0Å.

Frame Overlap
When the neutron bandwidth as limited by the bandwidth choppers is larger than that dictated by the frame time width, neutrons emitted from two consecutive pulses arrive at the detector in the same time frame.

Leakage
Neutrons with long wavelengths leak through the bandwidth choppers and arrive at the detector at a later time. The term ***leakage*** used in this document differs from that of ***frame overlap*** even though in both cases, neutrons of undesired wavelength arrive at the detector at the wrong time.

Chopper Window, Chopper Opening
The chopper window opening is assumed to be arc shaped, as shown in Figure 4. The opening angle refers to the arc angle of the window. The chopper ***open time*** or ***open period*** refers to the time interval when neutrons can pass through the chopper window.

Chopper Phase Delay
The time delay after the source neutron pulse before the chopper is opened.

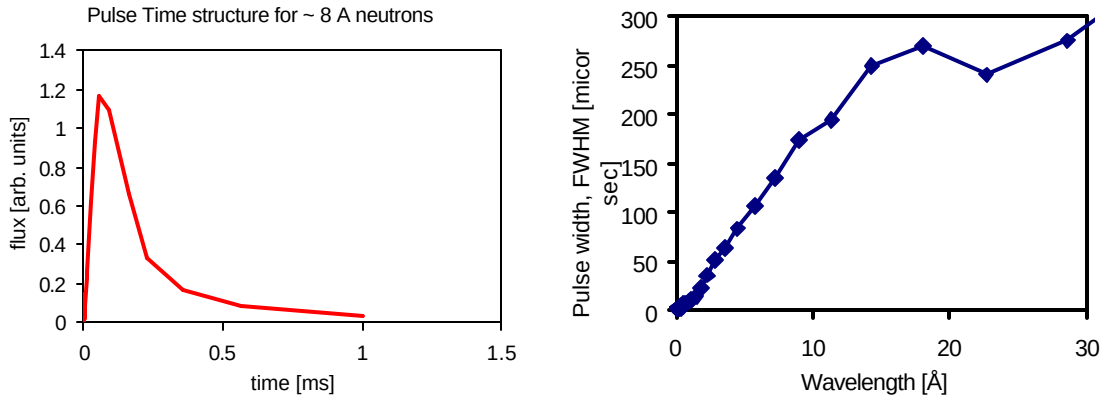

Figure 2. Initial neutron pulse structure for 8Å neutrons (left) and neutron pulse's FWHM as a function of wavelength (right) for the coupled liquid hydrogen moderator at the SNS. Data supplied by Eric Iverson SNS.

1.2 Initial Neutron Pulse Width

The initial neutron pulse from the downstream, upper, coupled hydrogen moderator of the high power target station of the SNS has a relatively long time tail. Figure 2 shows Monte-Carlo simulations of typical time structures of the source pulse and the pulse's full width half maximum (FWHM) as a function of the neutron wavelength. The simulation data are supplied by Eric Iverson of the SNS. For neutrons with wavelengths below ~15Å, the FWHM is approximately proportional to the neutron wavelength and is Δt ~ 20μs/Å. In this document, Δt =20μs/Å is assumed for all neutrons, including those with very long wavelengths. The variations in the actual FWHM for longer wavelength neutrons do not have any significant impact on the actual design choice for the choppers.

Unless otherwise noted, the calculations in this document use the value of Dt =20ms/Å as the pulse width. The pulse width is especially importance for neutron leakage tests. Wider pulses will be considered for the design of single choppers.

1.3 Umbra and Penumbra

Umbra and penumbrae originate from the fact that the initial neutron pulse has a finite time width. The definitions of umbra and penumbra that are used in this document are shown in Figure 3.

1.3.1 Frame Width

The frame time width is determined by the pulse repetition rate f of the neutron source. The frame wavelength width is primarily determined by the frame time width, with minimal contributions from the time width of the source pulse. If the width of the source pulse is neglected, *i.e.* $\Delta t=0$, the frame wavelength width, Δl, is given by:

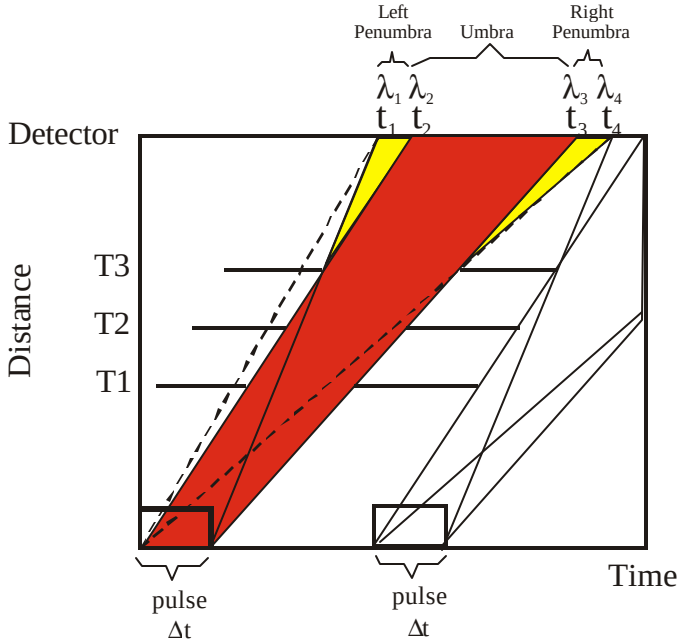

Figure 3. Definition of umbra (red area) and penumbrae (yellow areas). The T_3 chopper is used as the frame definition chopper. It limits both the umbra and penumbrae. The T_1 and T_2 choppers function as frame overlap elimination choppers in this context. For a given initial pulse width, T_1 and T_2 are opened to the edges of the umbra. The time period t_2-t_3 is the umbra while t_1-t_2 and t_3-t_4 are the left and the right penumbrae, respectively. The wavelength band for the umbra and penumbrae are l_1-l_2, l_2-l_3, and l_3-l_4, respectively. The dashed line indicates where the choppers would have to be opened to if the pulse width is $\Delta t=0$.

$$\Delta l = \frac{3956}{Lf}\,[\text{Å}] \tag{1}$$

Here, L is the location of the detector, or the distance of the detector from the neutron moderator, in [m]. The detector operation range of the EQ-SANS is L=15-25m[(i)]. f is the repetition rate or the neutron source, namely 60Hz for the high power target of the SNS.

When the source pulse width is considered, the total wavelength bandwidth (umbra+penumbrae) is modified to (Figure 3):

$$\Delta l = \frac{3956}{L}\left[\frac{1}{f}+\Delta t\cdot l_1\left(2-\frac{L}{L_{T_3}}\right)\right] \tag{2}$$

[(i)] The exact maximal detector-to-moderator distance will be determined by the actual engineering constraint. In all likelihood, it will be larger than the 18m as was in the conceptual design, and less or equal to 25m.

Here, Δt is the source pulse width per unit wavelength, in [s/Å]. λ_1 is the shortest wavelength in the frame, or the left boundary of the left penumbra. L_{T3} is the location of frame definition chopper, T_3.

1.3.2 Width of the Penumbrae

The time and wavelength widths of the left penumbra are given by (see Figure 3):

$$\Delta t_L = t_2 - t_1 = \Delta t \cdot l_1 \frac{L - L_{T_3}}{L_{T_3}} \tag{3}$$

$$\Delta l_L = l_2 - l_1 = 3956 \Delta t \cdot l_1 \frac{1}{L_{T_3}} \tag{4}$$

Similarly, the widths of the right penumbra are:

$$\Delta t_R = t_4 - t_3 = \Delta t \cdot l_3 \frac{L - L_{T_3}}{L_{T_3}} \tag{5}$$

$$\Delta l_R = l_4 - l_3 = 3956 \Delta t \cdot l_3 \frac{1}{L_{T_3}} \tag{6}$$

The quantities, L, Δt, λ_1, and L_{T3} are the same as those defined in equations (1) and (2). λ_3 is right wavelength boundary of the umbra.

1.3.3 Width of the Umbra

The time and wavelength widths of the umbra are given by (see Figure 3):

$$\Delta t_L = t_3 - t_2 = \frac{1}{f} - \Delta t \cdot (l_1 + l_3) \frac{L - L_{T_3}}{L_{T_3}}, \tag{7}$$

$$\Delta l = t_3 - t_2 = \frac{3956}{L}\left[\frac{1}{f} + 2\Delta t \cdot l_1\right] - \frac{3956}{L_{T_3}} \Delta t \left[2 l_1 + l_3\right] \tag{8}$$

The quantities, L, Δt, λ_1, λ_3, and L_{T3} are the same as those defined for the penumbrae.

1.3.4 Chopper phase delays and opening time intervals

For a minimum wavelength l_1 chosen for a wavelength frame, the phase delay of the frame definition chopper T_3, or the delay in time before the chopper opens up, is given by

$$t_0^{T_3} = \frac{L_{T_3}}{3956} l_1 + \Delta t l_1 \tag{9}$$

The quantities, Δt, λ_1, and L_{T3} are defined in the same say as those in the last section.

The *maximum* phase delays for the T_1 and T_2 choppers without limiting the umbra are:

$$t_0^{T_{1,2}} = \frac{L_{T_{1,2}}}{3956} l_2 \tag{10}$$

$L_{T1,2}$ is location of the T_1 or T_2 chopper.

The opening times, namely the time interval during which the choppers are open, are given by:

$$\Delta t_0^{T_{1,2,3}} = \frac{L_{T_{1,2,3}}}{L}\left(\frac{1}{f} - \Delta t_R\right) + \Delta t\, l_3\left(1 - \frac{L_{T_{1,2,3}}}{L_{T_3}}\right) \tag{11}$$

Δt_R is the time width of the right penumbra (equation 5).

In the following chapters, equations (9) and (10) are used to calculate the chopper phase delays. The additional, manual adjustments to the chopper phases referred in those chapters are given in values relative to those calculated by equations (9) and (10).

1.3.5 Chopper rising and falling times

The chopper rising and falling time is when the leading or the closing edge of the chopper cuts through the neutron beam. During these time periods, the neutron beam is partially open. The rising or falling time is given by

$$dt = \frac{w}{2pRf} \tag{12}$$

w is the width of the neutron beam. R is the radius of the inner edge of the chopper window. f is the rotation frequency of the chopper, which is the same as the source repetition rate (60Hz) under normal operation.

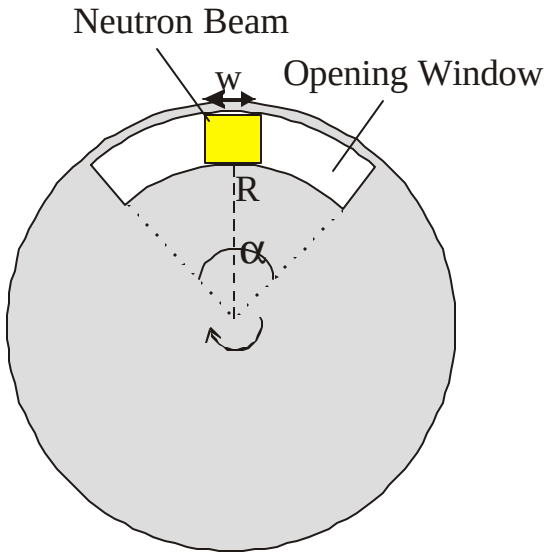

Figure 4. Schematics of a disk chopper cutting through the neutron beam.

Because of this chopper rising and closing times, the opening angles of the choppers have to be reduced accordingly to avoid frame overlaps and leakages of long wavelength neutrons. The angle correction is given by

$$da = \frac{w}{R} \tag{13}$$

For double-disk choppers, the rising time correction can be carried out at the run time. For single-disk choppers, this correction has to be incorporated in the chopper design.

The corrected chopper opening angles are reflected in the final design choices in chapter 2 only. The chopper opening angles in the rest of the chapters do not take equation (13) into account, because it is the chopper opening time, not its open angle that determines the calculations. The chopper opening times in those chapters can be considered as the total time period when the choppers let neutrons pass through, which includes the rising time given by (12).

2. Design Choice Summaries

This chapter summarizes the physics design of the three bandwidth choppers on the EQ-SANS. The location of the choppers are chosen such that the chopper system will cover the needs for all possible operation conditions on the EQ-SANS, namely between the detector-to-moderator distances of 15-25m (see note (i) on page 7) and in the first to fourth frames. With single-disk bandwidth choppers as included in the SNS project baseline for the EQ-SANS, the chopper window sizes have to be optimized around a particular detector location. In terms of enabling maximal neutron bandwidth without frame overlaps and eliminating neutron leakages, the chosen chopper window sizes in this chapter will perform best around the second frame with the collimation length of 4m, namely at the detector location of 18m, and without pulse rejection. This is an operational setup that will be extensively used on this instrument. The chopper designs are also tested against all other possible operational setups.

2.1 Chopper Locations

The three bandwidth choppers on the EQ-SANS are designed at **T_1 = 5.7m, T_2 = 7.8m, and T_3 = 9.5m** from the moderator, respectively.

In the case of double-disk choppers, we assume that the chopper window openings are adjusted dynamically to allow the maximum passage of the desired neutron band without causing overlaps of adjacent frames, namely the neutron bandwidth limited by the choppers is the same as that determined by the time frame at a chosen detector distance. These choppers will stop the leakage of all neutrons under ~35Å under all possible operation conditions of the EQ-SANS, namely, for detector-to-moderator distances between 15m and ~25m (see note (i) on page 7) and for first to fourth frame operations.

In the case of single-disk choppers, the sizes of the chopper windows have to be predetermined. We use chopper window sizes that are larger than that determined by the maximum detector distance of 25m and use the chopper phasings to limit the bandwidth when the detector is at larger distance (next section).

2.2 Single-Disk Chopper Opening Angles

The opening angles for the three single-disk bandwidth choppers are summarized in Table 1. These angles are based on the frame width values when the detector is at 18m and with the neutron pulse width ignored.

In Chapter 4, the chopper openings used for the calculations are based on the frame width values when the detector is at 17m. Those window sizes are the widest possible values that still allow the EQ-SANS to be operated at the detector distance of 25m. We base our final choices for the chopper window sizes on the frame width at 18m to provide more operational

margins and to better stop leakages from long delayed neutrons. More discussions are found in chapter 4.

The beam cross section on the EQ-SANS is 4cm wide. For a disk chopper with the radius of R = 30 cm, the beam cross section corresponds to an opening angle of 7.6°. These angle values are subtracted from those calculated using equation (11) in order to take the rising time of the choppers into account (Table 1).

Table 1. Locations and opening angles for the three bandwidth choppers. The chopper rising time correction is based on 30cm radius chopper disks.

Chopper	Location [m]	Chopper Window Opening Angel [°]	
		Without chopper rising time correction	With a 7.6° deduction for rising time correction
T1	5.7	114	**106.4**
T2	7.8	156	**148.4**
T3	9.5	190	**182.4**

3. Operation with Double-disk Choppers

Even though the bandwidth choppers for EQ-SANS included in the SNS project baseline are single disk ones, looking into the usage of double-disk choppers is important as well since it forms the basis for further studies. In this chapter, the designed chopper locations are tested against the usage of double-disk choppers with varying detector locations and neutron frames. Pulse rejection is also considered. As discussed in Chapter 1, we use 35Å as our upper wavelength criteria for neutron leakage tests. In each of these calculations, unless otherwise noted, the chopper windows are open as wide possible without causing overlaps of adjacent frames (see equation 11 and Figure 3).

Even though the chopper rising times are not considered for calculating the chopper open time intervals (equation 11), these opening times can be considered as the total time when the choppers are open to the neutron beam, including when the beam is partially open. In this regard, the rising time correction is only relevant when designing the actual chopper window. Thus, the rising time corrections are not included in this chapter and the chopper opening angles listed in this chapter are without the rising time correction.

3.1 60Hz operation

60Hz operation is the typical operation mode on the EQ SANS. The chopper designs are tested against three possible operational detector distances, 25m 18m and 15m (see note (i) on page 7). At each of these detector distances, the required chopper phases and opening times are listed in tables for the 1^{st}-4^{th} frame operations. The total neutron band and the umbra that are allowed by the choppers in each case are also listed. The time diagrams and neutron leakage plots for each of the operational conditions are given as well.

Unless otherwise noted, the chopper phases and opening times are obtained using equations (9-11). All the calculations for the chopper phases and opening angles as well as for neutron leakages use the neutron pulse width of 20ms/Å. The effects of broader pulses are considered in Chapter 4 only.

3.1.1 Detector at 25m

The detector distance of 25m is the maximum possible operational distance of the EQ-SANS under most likely scenarios (see note (i) on page 7). This section presents the operational conditions and leakage tests for this detector location.

As it is evident from the tables and plots below, with the designed locations for the choppers, there will be no leakages below the wavelength of 35Å in the 1^{st}-4^{th} frames at this distance.

Table 2. Chopper phases, openings, and neutron frame widths for the detector distance of 25m in the 1st-4th frames. The chopper phases ('Open At'), opening time intervals ('Open Duration'), opening angles, total wavelength band and the umbra are given. The given chopper opening angles are without the rising time correction. The variations in chopper openings between the frames are due to the finite time width of the initial pulse. The chopper phase is relative to time 0.

Frame No.	Chopper	Location [m]	Open At [ms]	Open Duration [ms]	Open Angel [°]	Frame Width [Å]	Umbra [Å]
1	T1	5.7	1.4528	3.8020	82.1236	1-3.627	1.008-3.597
	T2	7.8	1.9881	5.1762	111.8059		
	T3	9.5	2.4214	6.2886	135.8344		
2	T1	5.7	3.8316	3.8029	82.1432	2.637-5.27	2.659-5.226
	T2	7.8	5.2433	5.1655	111.5748		
	T3	9.5	6.3861	6.2685	135.4004		
3	T1	5.7	7.6633	3.8044	82.1748	5.275-7.915	5.319-7.849
	T2	7.8	10.4866	5.1483	111.2026		
	T3	9.5	12.7722	6.2362	134.7013		
4	T1	5.7	11.4949	3.8058	82.2064	7.912-10.561	7.978-10.473
	T2	7.8	15.7299	5.1310	110.8304		
	T3	9.5	19.1582	6.2038	134.0022		

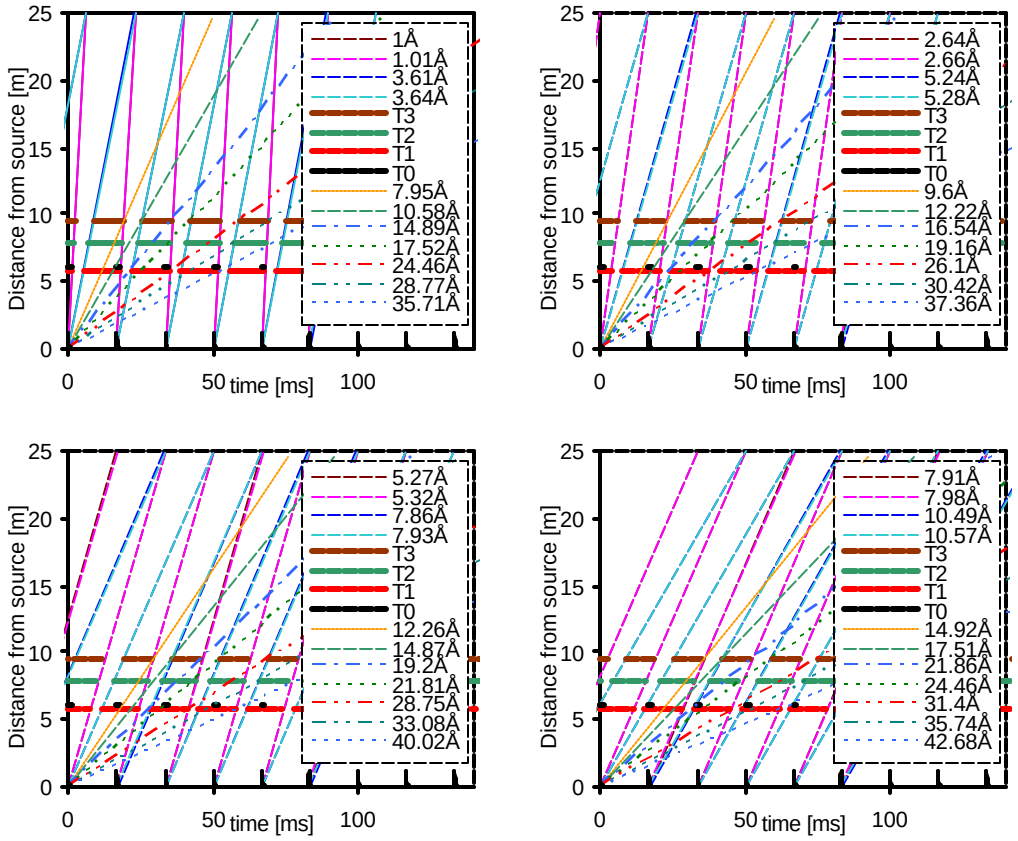

Figure 5. Time diagram for the detector distance of 25m, 1st-4th frames (1st: top-left, 2nd: top-right, 3rd: bottom-left, 4th: bottom-right). The chopper phases and opening times are as listed in Table 2. The thick, horizontal lines indicate the choppers. The thin solid lines are the boundaries for the umbra and penumbrae (see Figure 3). Due to the small pulse width of 20ms/Å, the penumbrae are not very discernible in the plot. To indicate the blockage of slower neutrons, neutrons that arrive at the time when the choppers are opened or closed in higher frames are drawn as thin dotted or dashed lines. The emission time of these slower neutrons is set to 0.

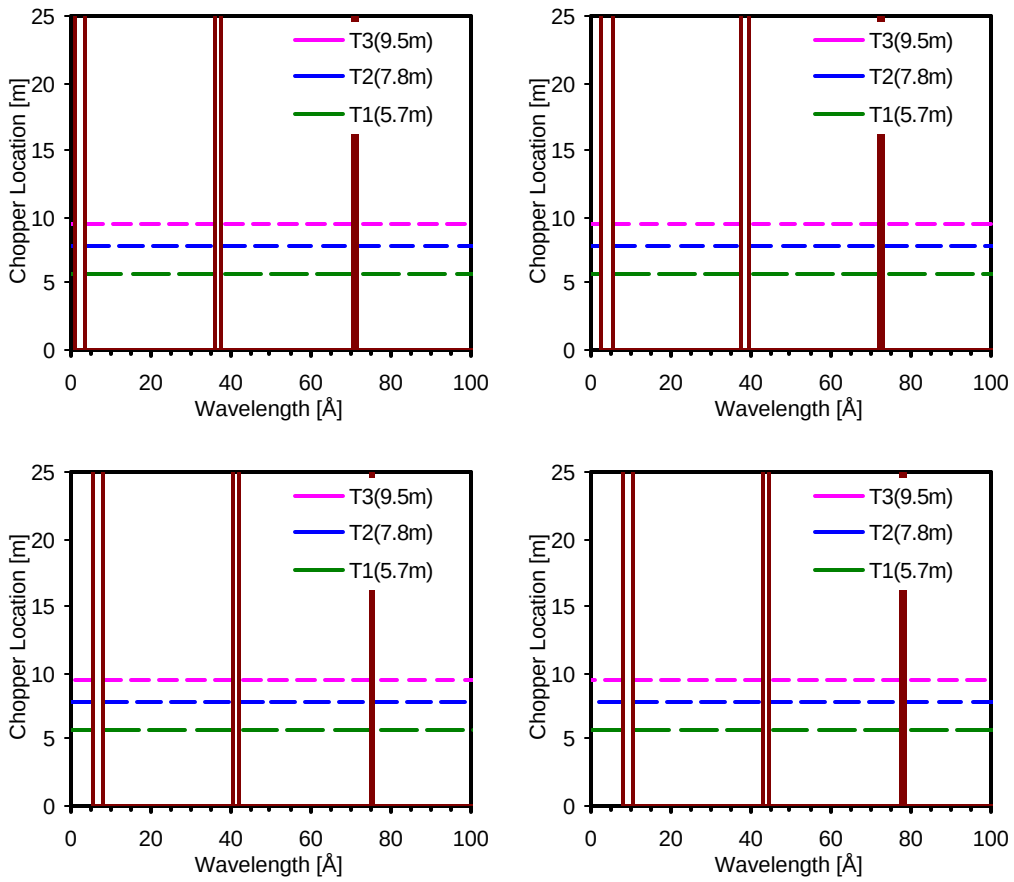

Figure 6. Neutron band passes through the chopper system in the 1st-4th frames (1st: top-left, 2nd: top-right, 3rd: bottom-left, 4th: bottom-right) for the detector distance of 25m. The chopper phases and opening times are as listed in Table 2. Neutrons that are emitted up to 20ms/Å after time 0 are considered for these leakage tests. The dashed, horizontal lines indicate the neutron wavelength bands that each chopper blocks (closed) or allows (open) to pass. The vertical lines indicate neutrons that pass all three choppers. Two vertical lines without a chopper blockage in between define the boundaries of a passing neutron band. In all 4 frames, no neutron leakage is seen below ~35Å.

3.1.2 Detector at 18m

This section shows the operational conditions, time diagrams and neutron leakage plots for the detector location of 18m. The conditions for the calculations and tests are the same as for the last section. No neutron leakages below 35Å under all operational conditions at this detector distance are seen.

Table 3. Chopper phases, openings, and neutron frame widths for detector at 18m. See Table 2 for explanation.

Frame No.	Chopper	Location [m]	Open At [ms]	Open Duration [ms]	Open Angel [°]	Frame Width [Å]	Umbra [Å]
1	T1	5.7	1.4528	5.2886	114.2331	1-4.653	1.008-4.614
	T2	7.8	1.9881	7.2029	155.5829		
	T3	9.5	2.4214	8.7526	189.0566		
2	T1	5.7	5.3217	5.2947	114.3662	3.663-7.328	3.693-7.266
	T2	7.8	7.2824	7.1919	155.3446		
	T3	9.5	8.8696	8.7277	188.5176		
3	T1	5.7	10.6435	5.3032	114.5494	7.326-11.007	7.387-10.915
	T2	7.8	14.5647	7.1767	155.0169		
	T3	9.5	17.7391	8.6933	187.7763		
4	T1	5.7	15.9652	5.3117	114.7326	10.989-14.686	11.08-14.563
	T2	7.8	21.8471	7.1615	154.6891		
	T3	9.5	26.6087	8.6590	187.0349		

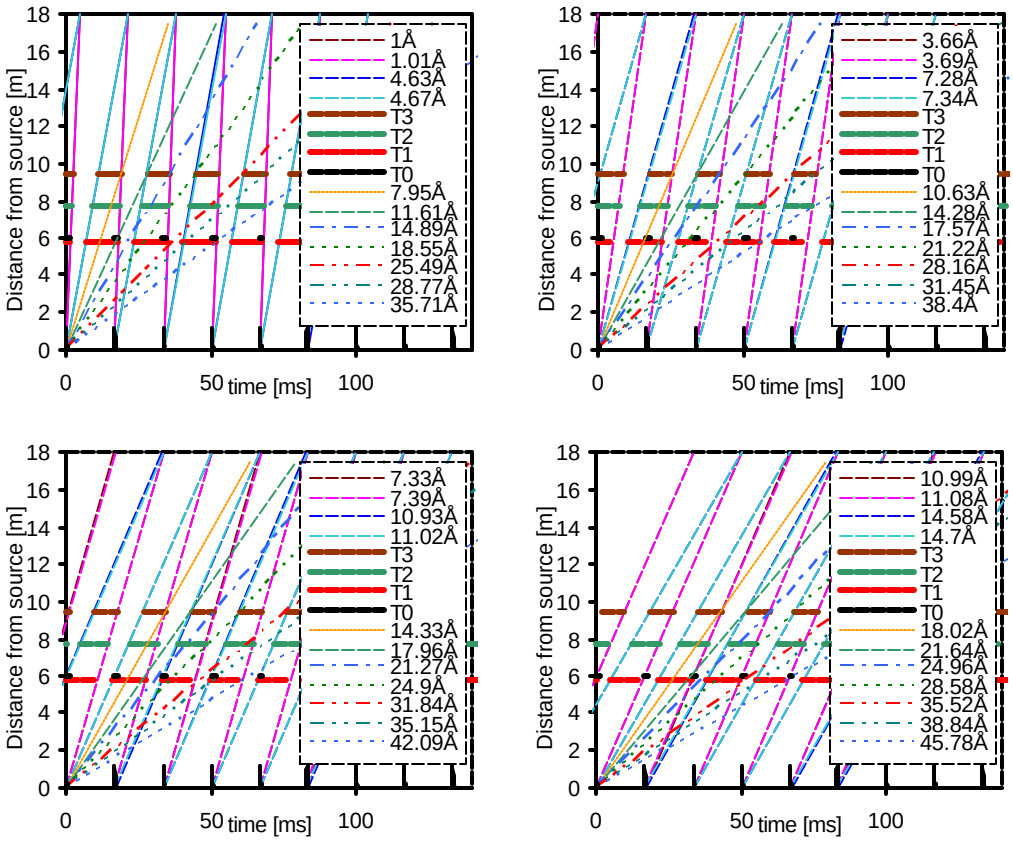

Figure 7. Time diagram for the detector location of 18m, in the 1st-4th frames (1st: top-left, 2nd: top-right, 3rd: bottom-left, 4th: bottom-right). The chopper phases and opening times are as listed in Table 3. See Figure 5 for explanation.

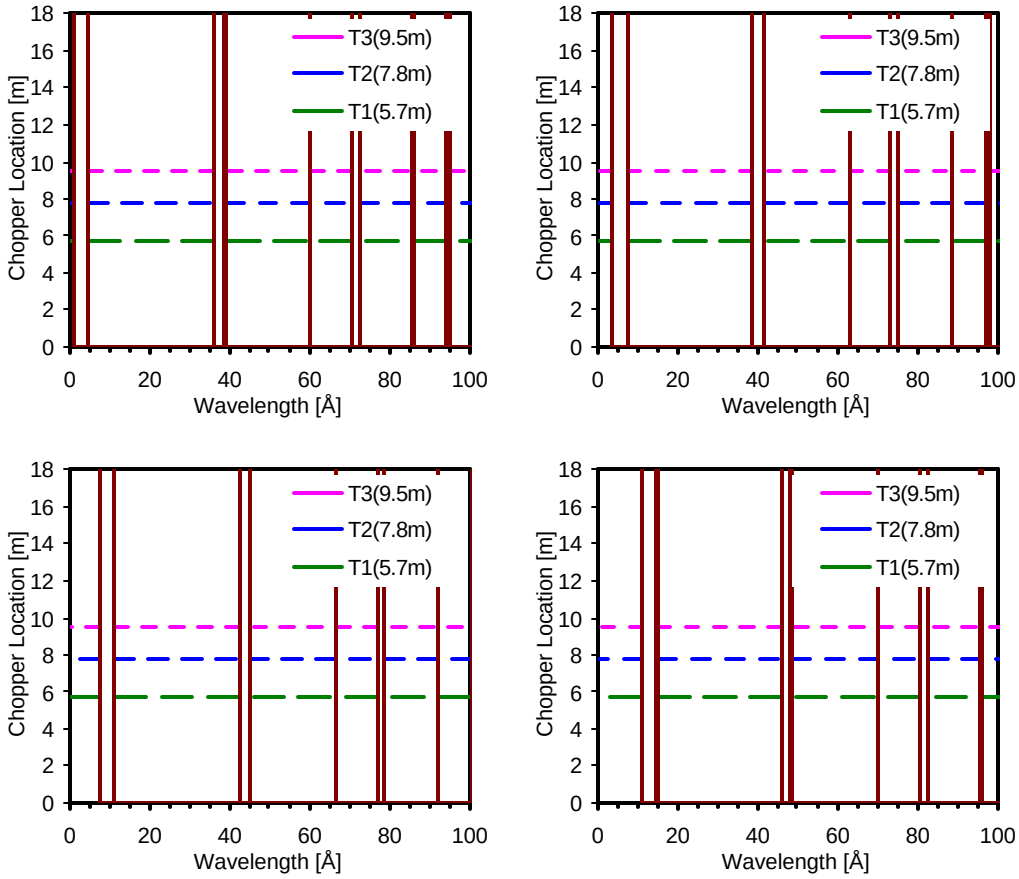

Figure 8. Neutron band pass through the chopper system in the 1st-4th frames (1st: top-left, 2nd: top-right, 3rd: bottom-left, 4th: bottom-right) for the detector distance of 18m. The chopper phases and opening times are as listed in Table 3. See Figure 6 for explanation.

3.1.3 Detector at 15m

The detector location of 15m is the shortest detector to moderator distance designed for the EQ-SANS. In this section, the operational conditions for the choppers are shown.

Table 4. Chopper Phases, opening times, and frame widths for detector at 15m. See Table 2 for explanation.

Frame No.	Chopper	Location [m]	Open At [ms]	Open Duration [ms]	Open Angel [°]	Frame Width [Å]	Umbra [Å]
1	T1	5.7	1.4528	6.3526	137.2162	1-5.388	1.008-5.342
	T2	7.8	1.9881	8.6536	186.9176		
	T3	9.5	2.4214	10.5163	227.1521		
2	T1	5.7	6.3861	6.3648	137.4787	4.396-8.801	4.432-8.727
	T2	7.8	8.7388	8.6454	186.7396		
	T3	9.5	10.6435	10.4916	226.6176		
3	T1	5.7	12.7722	6.3805	137.8184	8.791-13.22	8.864-13.109
	T2	7.8	17.4777	8.6347	186.5092		
	T3	9.5	21.2869	10.4595	225.9256		
4	T1	5.7	19.1582	6.3962	138.1581	13.187-17.639	13.296-17.491
	T2	7.8	26.2165	8.6240	186.2787		
	T3	9.5	31.9304	10.4275	225.2336		

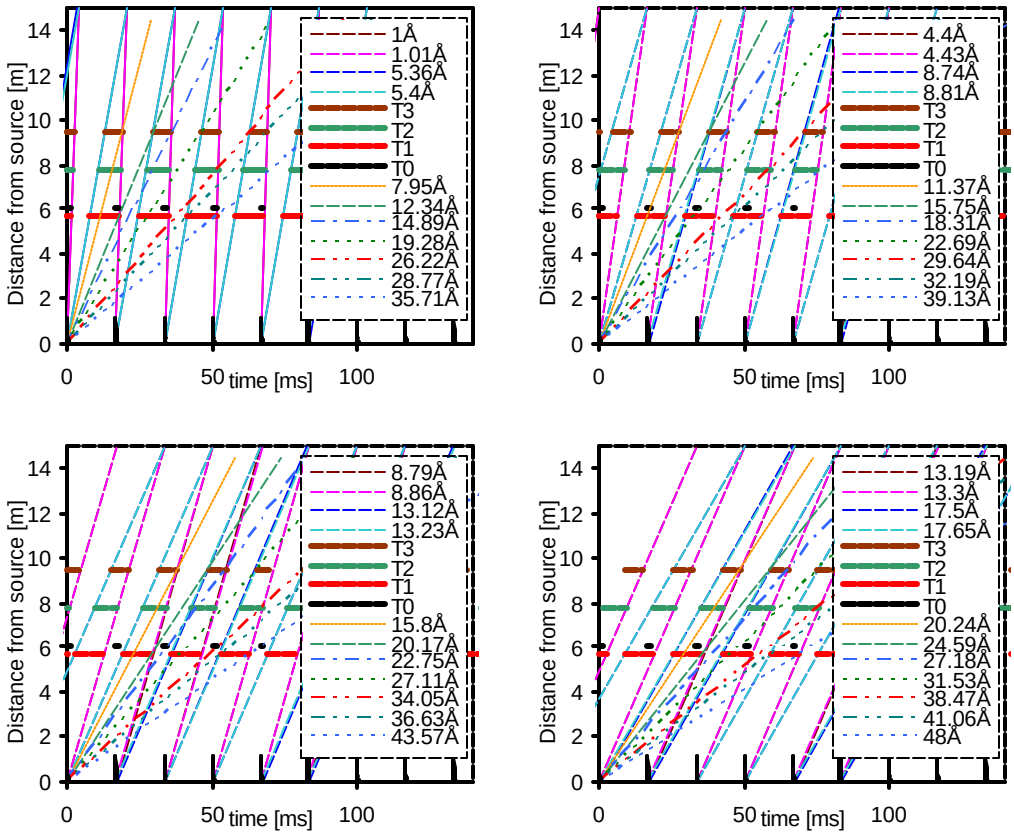

Figure 9. Time diagram for the detector distance of 15m in the 1st-4th Frames (1st: top-left, 2nd: top-right, 3rd: bottom-left, 4th: bottom-right). The chopper phases and opening times are as listed in Table 4. See Figure 5 for explanation.

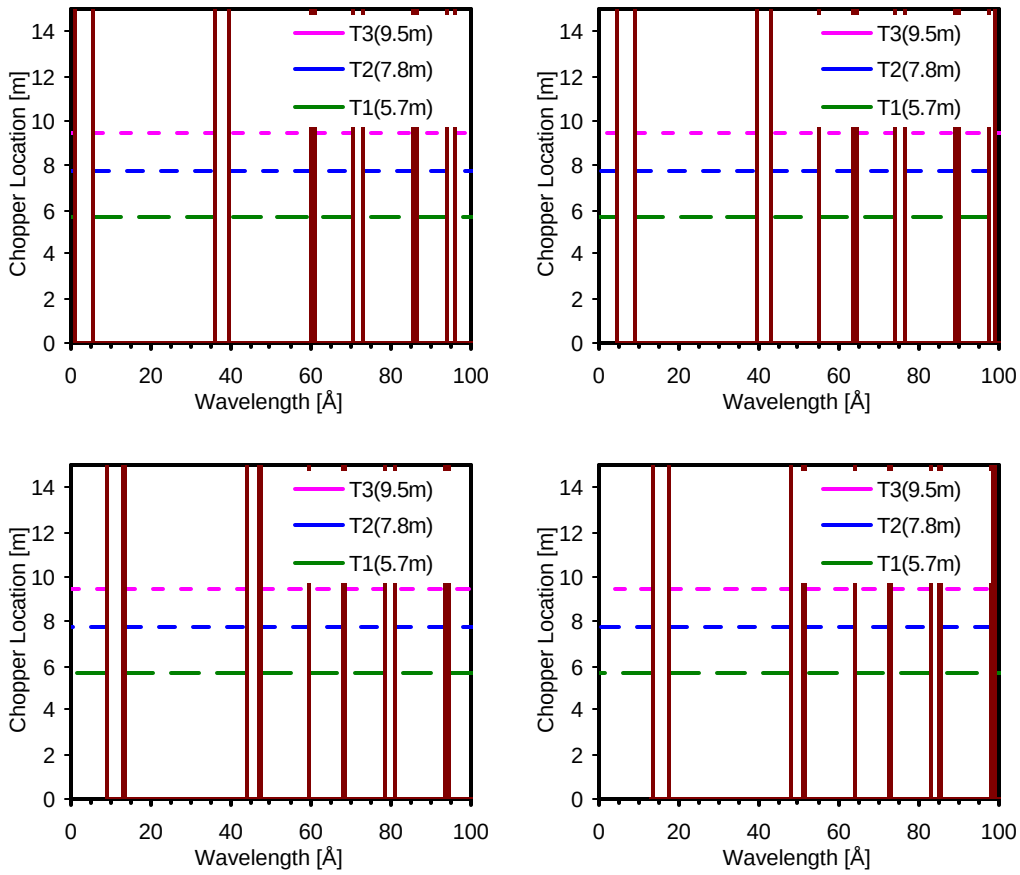

Figure 10. Neutron band pass through the chopper system in the 1st-4th frames (1st: top-left, 2nd: top-right, 3rd: bottom-left, 4th: bottom-right) for the detector distance of 15m. The chopper phases and open time periods are as listed in Table 4. See Figure 6 for figure explanation.

3.2 Pulse Rejection, 30Hz Operation

Pulse rejection is not a typical mode of operation on the EQ-SANS. However studying the feasibility of pulse rejection on this instrument is still useful if users choose to run the instrument in this mode. When every other neutron pulses from the source are rejected by the chopper system, the neutron frame width will be twice that of normal 60Hz operation. However, if the disk choppers are opened wide enough to allow this neutron band, there will be leakages from the rejected pulses through the choppers around 15-20Å for all operational detector distances (15-25m). To eliminate these leakages, the *maximum* neutron bandwidth has to be reduced to ~ 4.6Å by adjusting the choppers, regardless of the detector location. This is demonstrated in the following discussions for the detector distances of 25m, 18m, and 15m. Thus, the effective use of the pulse rejection will be at the largest detector distance of 25m on this instrument. The wider neutron wavelength band that would have been allowed by the time frame at shorter detector distances cannot be used.

3.2.1 Detector at 25m

At the 25m detector distance, if the three bandwidth choppers are opened as wide as the frame width allows, there will be a leakage at ~14.2Å from the rejected pulses (figure 11).

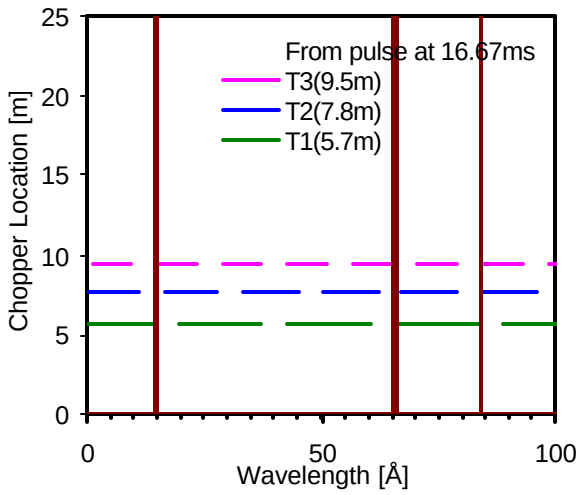

Figure 11. Neutron leakages from the rejected pulse for the detector distance of 25m in the second to third frames (see Figure 6 for figure explanation). The choppers are wide open to allow maximum neutron band passage without overlaps of adjacent frames. The leakage below 35Å occurs ~ 14.2Å.

To remove the leakage at ~14.2Å, the allowed frame width by the choppers has to be reduced either by reducing the chopper openings or by changing the relative phases between the choppers. For the calculations in the following, the T_1 chopper is closed for an extra time of 1ms. , namely T_1 is remain closed 1ms more than that calculated by equation (11). This T_1 chopper closedown removes the leakages from the rejected pulse.

The extra 1m closedown of the T1 chopper reduces the neutron bandwidth from the maximum frame width of 5.3Å at this distance to 4.6Å.

Table 5. Chopper operation with pulse rejection at the detector distance of 25m. See Table 2 for explanation. The T_1 chopper opening time is reduced by an extra 1ms from the values calculated using equation (11).

Frame No.	Chopper	Location [m]	Open At [ms]	Open Duration [ms]	Open Angel [°]	Frame Width [Å]	Umbra [Å]
2-3	T1	5.7	4.8316	6.6431	71.7455	3.317-7.92	3.353-7.854
	T2	7.8	5.2433	10.4012	112.3331		
	T3	9.5	6.3861	12.6340	136.4468		

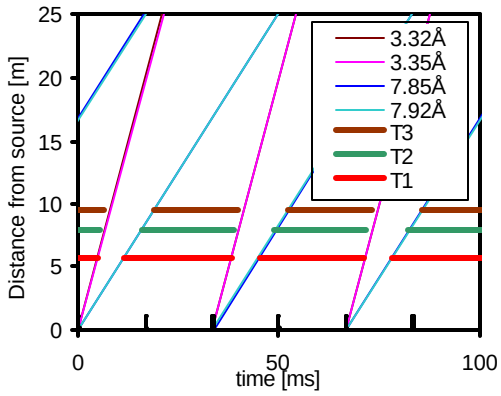

Figure 12. Time diagram with one pulse rejection at the detector distance of 25m in the second to third frames. See Figure 5 for explanation. The chopper phases and open time periods are as listed in Table 5.

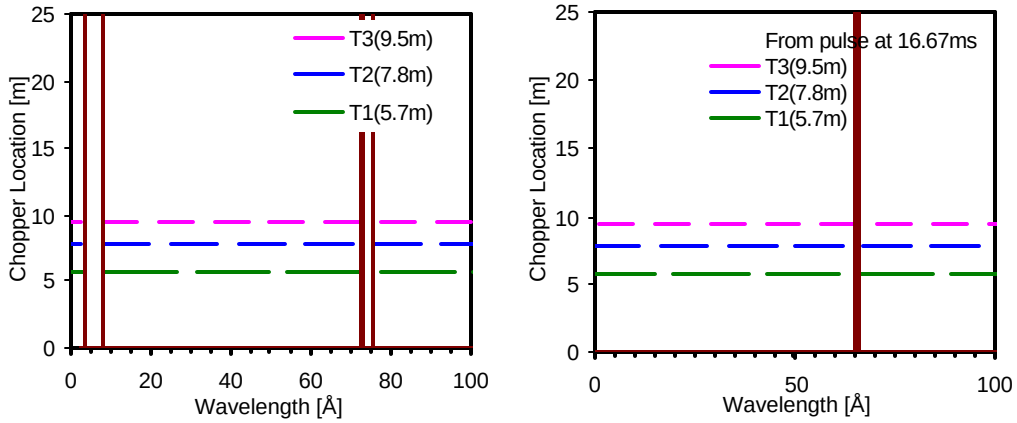

Figure 13. Neutron band pass from the chosen (left) and rejected (right) pulses for the second-third frame operation when the detector is at 25m. See Figure 6 for explanation. The chopper phases and opening times are as listed in Table 5. Leakages from the rejected pulses (figure 11) are now removed.

3.2.2 Detector at 18m

At the detector distance of 18m, if the three bandwidth choppers are opened as wide as the frame width allows, the leakage from the rejected pulse occurs between ~15-18Å (Figure 14).

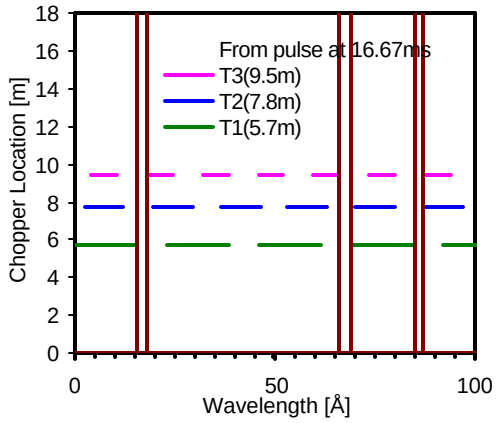

Figure 14. Neutron leakages from the rejected pulse for the detector distance of 18m for the second-third frame operation. See Figure 6 for explanation. The choppers are wide open to allow maximum neutron band passage without overlaps of adjacent frames. Neutrons with the wavelength of ~15-18Å from the rejected pulse leak through the chopper system.

Similar to the discussions in the last section for the detector distance of 25m, the T_1 chopper closedown required for T1 is ~4ms. This reduces the neutron bandwidth to ~ 4.6Å from the maximum frame width of 7.3Å at this distance.

Table 6. Chopper operation with pulse rejection at the detector distance of 18m. See Table 2 for explanation. The T_1 chopper is closed for an extra 3.97ms from the values calculated using equation (11).

Frame No.	Chopper	Location [m]	Open At [ms]	Open Duration [ms]	Open Angel [°]	Frame Width [Å]	Umbra [Å]
2-3	T1	5.7	9.2917	6.6520	71.8415	6.398-11.005	6.449-10.913
	T2	7.8	7.2824	14.4550	156.1145		
	T3	9.5	8.8696	17.5580	189.6264		

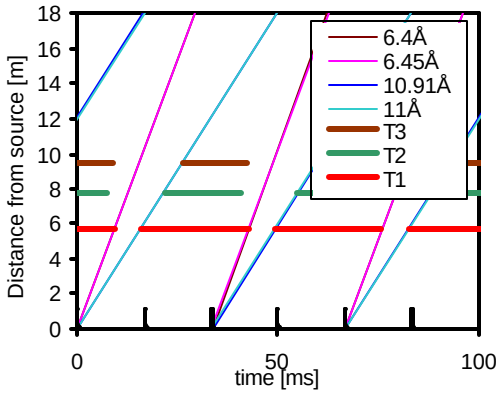

Figure 15. Time diagram with one pulse rejection at 18m in the second-third frames. See Figure 5 for explanation. The chopper phases and opening times are as listed in Table 6. Due to the effective closing down of the neutron frame through T_1 delay, there is a substantial time period on the detector when there are no neutrons arrive.

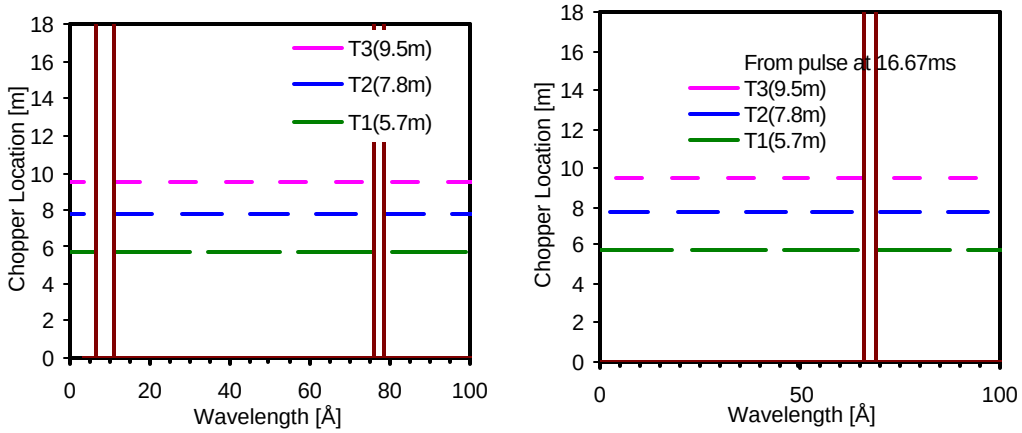

Figure 16. Neutron band pass from the chosen (left) and rejected (right) pulses for the second-third frame operation when the detector is at 18m. See Figure 6 for explanation. The chopper phases and open time perids are as listed in Table 6. Leakages from the rejected pulses (Figure 14) are now removed.

3.2.3 Detector at 15m

At the detector distance of 15m, the neutron leakage band from the rejected pulse is at ~16-20Å (figure 17, left) if the three bandwidth choppers are opened as wide as the frame width allows. In addition, if 2^{nd}-3^{rd} frames are used, there will be a leakage from the rejected pulse at short wavelengths (<1.7Å, figure 17, left). To stop the leakage at 16-20Å, the T_1 chopper has to be closed down by an extra time of ~6.1ms. The neutron leakage below 1.7Å cannot be stopped unless the bandwidth is further reduced (data not shown).

Table 7. Chopper operation with pulse rejection at the detector distance of 15m. See Table 2 for explanation. The T_1 chopper is closed for an extra 6.1ms from the values calculated using equation (10).

Frame No.	Chopper	Location [m]	Open At [ms]	Open Duration [ms]	Open Angel [°]	Frame Width [Å]	Umbra [Å]
2-3	T1	5.7	12.4861	6.6520	71.8418	8.605-13.21	8.666-13.099
	T2	7.8	8.7388	17.3537	187.4200		
	T3	9.5	10.6435	21.0789	227.6519		

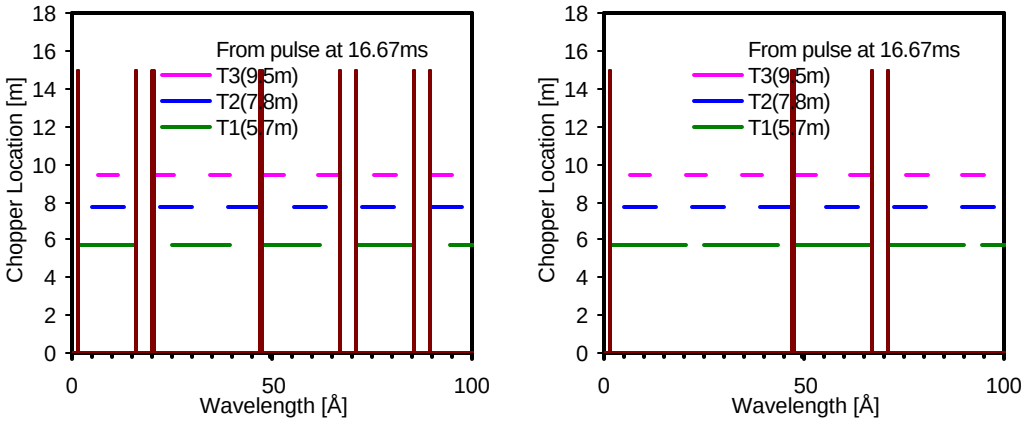

Figure 17. Neutron leakages from the rejected pulses in the second frame at 15m. See Figure 6 for explanation. Left: all the choppers are phased to allow maximum neutron bandwidth in the desired frame. Right: the T_1 chopper remains closed for an exta 6.1ms when compared to the left diagram (see Table 7). The leakages between 16-20 Å in the left diagram are removed on the right. However, there are still leakages below 1.7Å which would require further chopper closedowns to remove this leakage.

3.3 Two-Pulse Rejection

When two out of three neutron pulses are rejected, the leakages from the rejected pulses can no longer be stopped by the chopper system without having to reduce the chopper openings so much that any bandwidth benefit of pulse rejection is lost (Figure 18). Thus, the two-pulse rejection mode of operation on the EQ-SANS is not feasible.

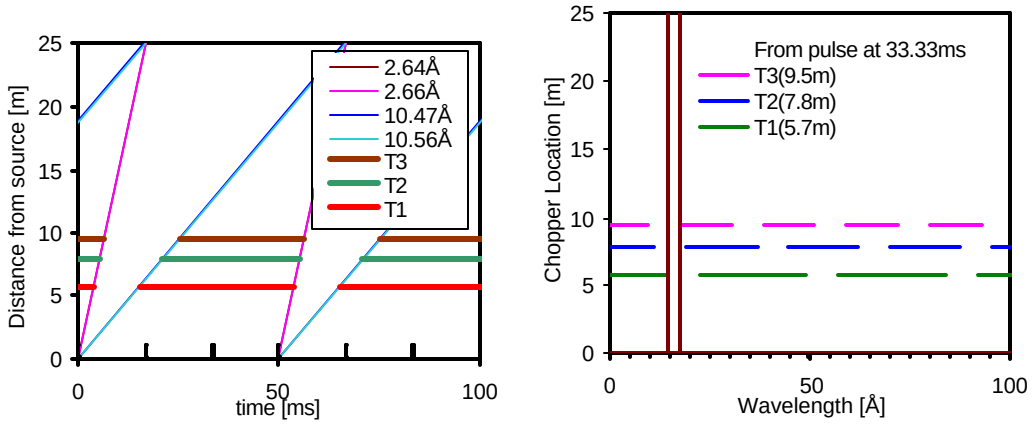

Figure 18. Time diagram (left) and leakage plot from the second rejected pulse (right) with two-pulse rejection (2nd–4th frame, 25 m). See Figures 5 and 6 for explanation. The leakages between 14.2-17.5Å from the rejected pulse at 33.33 ms can not be removed by adjusting the choppers.

4. All Single-disk Choppers

Single-disk choppers are included in the SNS project baseline for the EQ-SANS. This chapter considers the single-disk chopper designs and tests these designs against various operational conditions.

4.1 Chopper Window Opening Angles

With single-disk choppers, the sizes or angles of the chopper opening windows have to be pre-determined. Since the width of the neutron frames as determined by the detector location is inversely proportional the detector to moderator distance, one could conservatively use the smallest openings, namely those that correspond to the frame width when the detector is at its maximum distance of 25m (see note (i) on page 7) when designing the chopper disks. Such a design will ensure that there are no overlaps between adjacent frames at all detector locations. However, it will also severely reduce the amount of neutrons available when the detector is located closer to the moderator.

An alternative way is to have larger chopper windows and use the relative phasing between the choppers to reduce the frame width when the detector is at larger distances. The widest possible chopper openings turn out to be those that correspond to the frame width as defined by the detector location of 17m. With even wider chopper openings, namely those that correspond to the frame width at the detector distances of 15-16m, the chopper phases can no longer be adjusted for operations at the larger distance of 25m without having neutrons leaking into higher frames at the same time.

In this chapter, we use chopper openings as determined by the frame width at the detector distance of 17m to test the operations of the choppers at greater detector distances. Wider source neutron pulses and operations with pulse rejections are also considered. The final choices for the chopper windows in chapter 2 are slightly smaller, which provide more operational margins for stopping leakages of long delayed neutrons.

Table 8. Chopper opening time duration and angles used in this chapter. The values are based on the width of the second frame when the detector is at 17m. The source pulse width used in the calculation is 20μs/Å. Chopper rising time correction are not included in these values.

Chopper	Location [m]	Open Duration [ms] (60Hz)	Open Angel [°]
T1	5.7	5.6293	121.5922
T2	7.8	7.6465	165.1645
T3	9.5	9.2795	200.4373

4.2 60Hz Operation

60Hz is the typical operation mode on the EQ SANS. The designs of the single-disk choppers are tested here against operations at detector distances greater than 17m in the 1^{st}-4^{th} frames.

The reduction in neutron frame width is achieved by changing the relative phases between the choppers. *These phases are often not unique, namely different sets of chopper phases could some times be used to achieve the same performance.*

4.2.1 Detector at 25m

Table 9 summarizes the chopper phase shifts that are needed for operations at the detector distance of 25m. From the time diagrams (figure 19) and neutron leakage plots (figure 20), no leakages below ~ 35 Å in the 1^{st}-4^{th} frames are seen.

Table 9. Chopper phases required for operation at the detector distance of 25m. The frame widths as limited by the choppers are also listed.

Frame No.	Chopper	Location [m]	Open At [ms]	Frame Width [Å]	Umbra [Å]
1	T1	5.7	16.3202	1.003-3.624	1.013-3.593
	T2	7.8	1.9975		
	T3	9.5	16.0892		
2	T1	5.7	2.0323	2.637-5.275	2.664-5.231
	T2	7.8	5.2527		
	T3	9.5	3.3872		
3	T1	5.7	5.8323	5.275-7.912	5.328-7.845
	T2	7.8	10.5055		
	T3	9.5	9.7205		
4	T1	5.7	9.6323	7.912-10.549	7.992-10.446
	T2	7.8	15.7582		
	T3	9.5	16.0538		

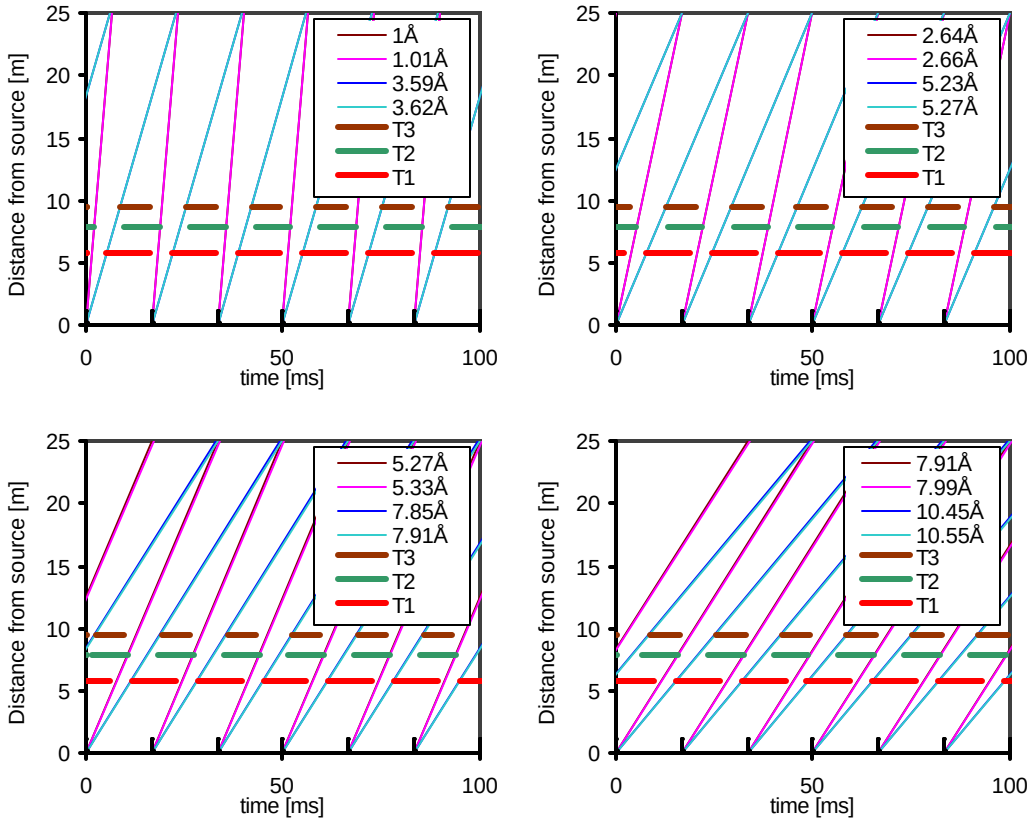

Figure 19. Time diagram for the detector distance of 25m, 1st-4th frames (1st: top-left, 2nd: top-right, 3rd: bottom-left, 4th: bottom-right). See Figure 5 for explanation. The chopper phases are as listed in Table 9. The phase shifts of the choppers are visible in the diagram.

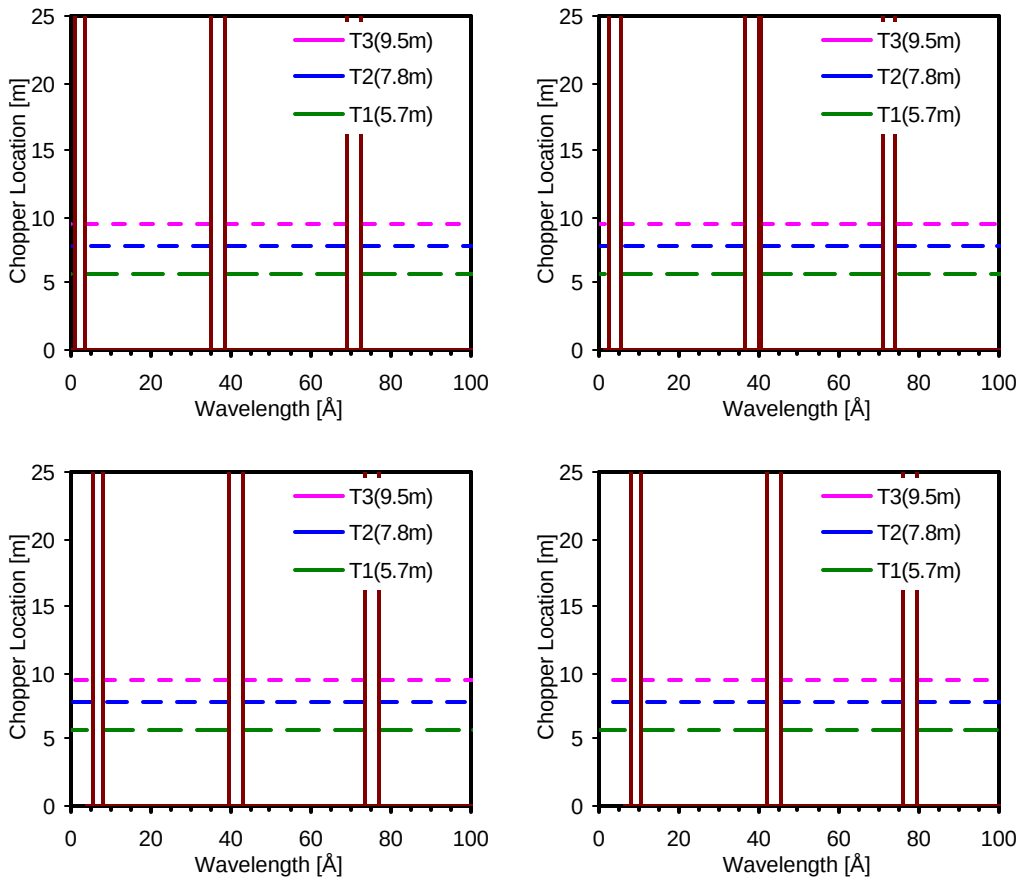

Figure 20. Neutron band passes through the bandwidth choppers in the first to fourth frames (1st: top-left, 2nd: top-right, 3rd: bottom-left, 4th: bottom-right) when the detector is at 25m. See Figure 6 for figure explanation. The chopper phases are as listed in Table 9.

4.2.2 Detector at 19-23m

In the last section, the chopper designs are tested against operations at the detector distance of 25m. At shorter detector distances, the operation of the choppers should pose lesser a problem than at 25m. This section lists the chopper phases that are needed to operate the EQ-SANS at the detector distance of 19m, 21m, and 23m. There are no neutron leakages below 35Å.The time diagrams and the neutron band pass plots are shown for the second frame only.

Table 10. Chopper phases required for operation at the detector distance of 19m. The frame widths limited by the choppers are also listed.

Frame No.	Chopper	Location [m]	Open At [ms]	Frame Width [Å]	Umbra [Å]
1	T1	5.7	0.8435	1.004-4.45	1.015-4.412
	T2	7.8	2.0005		
	T3	9.5	1.4058		
2	T1	5.7	4.4323	3.47-6.94	3.505-6.883
	T2	7.8	6.9115		
	T3	9.5	7.3872		
3	T1	5.7	9.4323	6.94-10.411	7.011-10.309
	T2	7.8	13.8230		
	T3	9.5	15.7205		
4	T1	5.7	14.4323	10.411-13.881	10.516-13.731
	T2	7.8	20.7345		
	T3	9.5	24.0538		

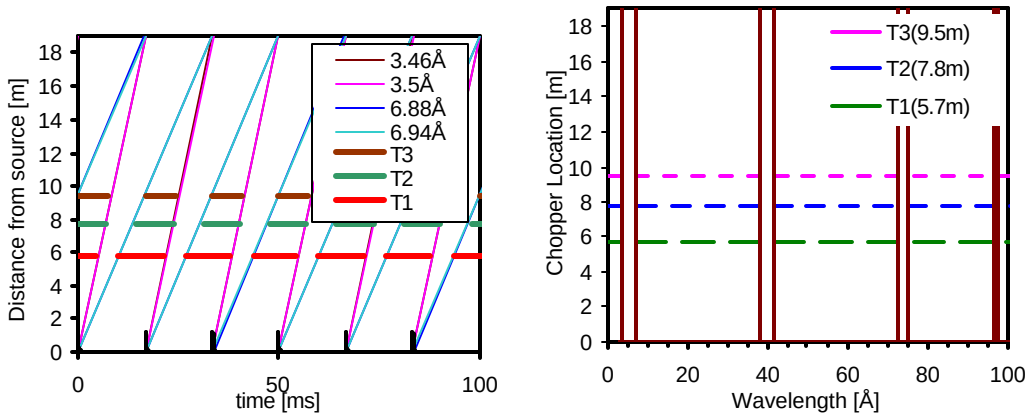

Figure 21. Time diagram (left) and the leakage plot (right) in the second frame at the detector distance of 19m (see Figures 5 and 6 for figure explanation). The chopper phases are as listed in Table 10.

Table 11. Chopper phases required for operation at the detector distance of 21m. The frame widths limited by the choppers are also listed.

Frame No.	Chopper	Location [m]	Open At [ms]	Frame Width [Å]	Umbra [Å]
1	T1	5.7	0.3713	1.004-4.122	1.014-4.087
	T2	7.8	1.9993		
	T3	9.5	0.6188		
2	T1	5.7	3.4799	3.14-6.279	3.172-6.227
	T2	7.8	6.2533		
	T3	9.5	5.7999		
3	T1	5.7	8.0037	6.279-9.419	6.343-9.331
	T2	7.8	12.5065		
	T3	9.5	13.3395		
4	T1	5.7	12.5275	9.402-12.559	9.497-12.427
	T2	7.8	18.7261		
	T3	9.5	20.8792		

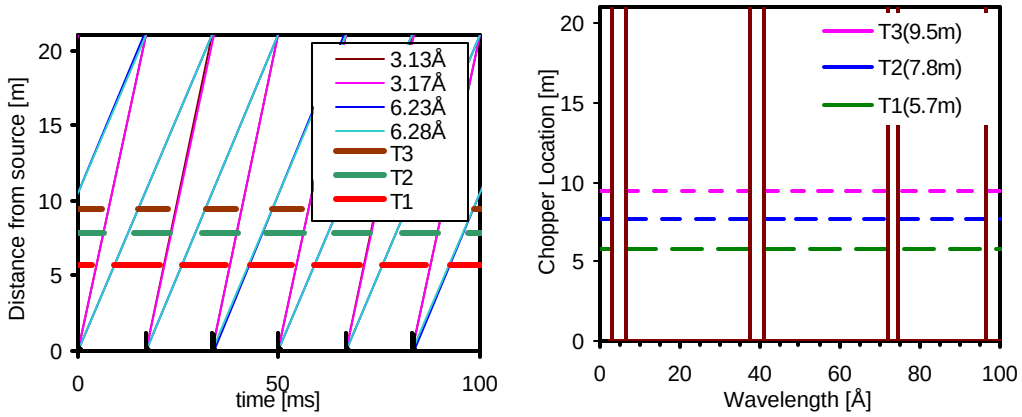

Figure 22. Time diagram (left) and the leakage plot (right) in the second frame at the detector distance of 21m (see Figures 5 and 6 for figure explanation). The chopper phases are as listed in Table 11.

Table 12. Chopper phases required for operation at the detector distance of 23m. The frame widths limited by the choppers are also listed.

Frame No.	Chopper	Location [m]	Open At [ms]	Frame Width [Å]	Umbra [Å]
1	T1	5.7	16.6478	1.003-3.851	1.014-3.819
	T2	7.8	1.9984		
	T3	9.5	16.6353		
2	T1	5.7	2.6932	2.867-5.733	2.896-5.686
	T2	7.8	5.7095		
	T3	9.5	4.4886		
3	T1	5.7	6.8236	5.733-8.6	5.791-8.523
	T2	7.8	11.4190		
	T3	9.5	11.3727		
4	T1	5.7	10.9540	8.6-11.467	8.687-11.35
	T2	7.8	17.1285		
	T3	9.5	18.2567		

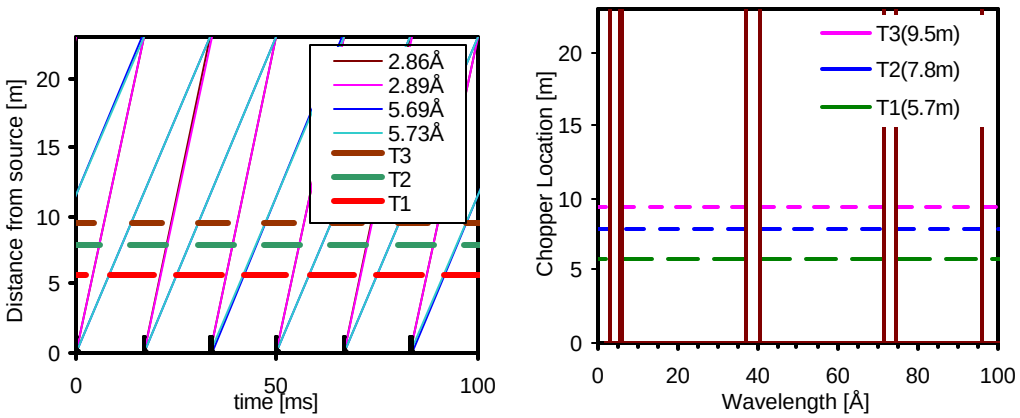

Figure 23. Time diagram (left) and the leakage plot (right) in the second frame at the detector distance of 23m (see Figures 5 and 6 for figure explanation). The chopper phases are as listed in Table 12.

4.3 Long delayed neutrons

Unlike the case of using double-disk choppers, where the window openings can be adjusted at the run time to stop the leakage from long delayed neutrons, the designed windows of the single-disk choppers have to be checked against leakages for wider pulses. The calculations thus far were carried out using the initial neutron pulse width of 20μs/Å. However, it is obvious that the choppers will have to be able to perform for wider pulses since a large fraction of neutrons are emitted after the pulse's 20μs/Å FWHM (figure 2).

With the opening windows as listed in Table 8, the chopper can be phased to stop neutrons that are long delayed. Table 13 lists the phases of the choppers that will stop leakage of

neutrons that are delayed up to 10x the source pulse FWHM (200μs/Å) in the second frame at the detector distance of 25m. The time diagram and leakage plot are shown following the table.

Table 13. Re-adjusted chopper phases to stop the leakage of neutrons that are delayed up to 10x the pulse FWHM (200μs/Å) for the detector distance of 25m in the second frame.

Frame No.	Chopper	Location [m]	Open At [ms]	Frame Width [Å]	Umbra [Å]
2	T1	2.0323	5.6293	2.589-5.275	2.857-4.593
	T2	5.6331	7.6465		
	T3	3.3872	9.2795		

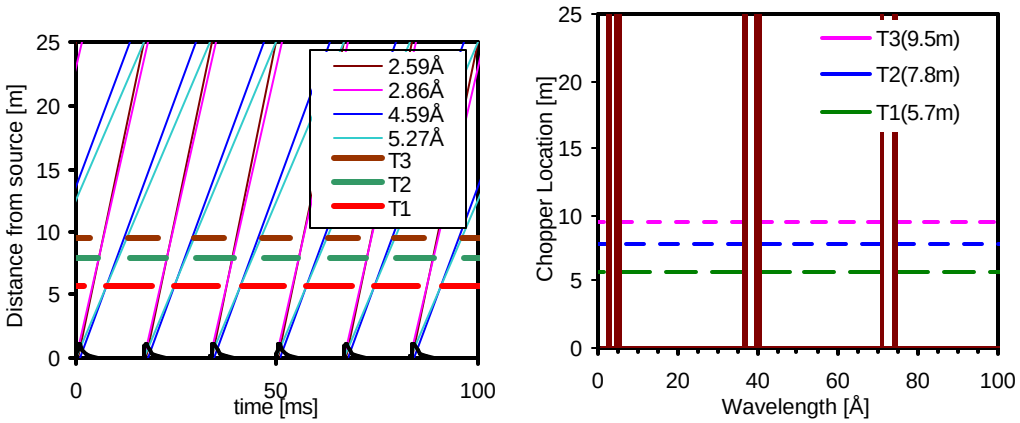

Figure 24. Time diagram (left) and neutron band pass through the bandwidth choppers (right) in second frame for the detector distance of 25m. See Figures 5 and 6 for figure explanation. The chopper phases are as shown in Table 13. The leakages are calculated with the pulse width of 200 μs/Å. The right penumbra (thin blue and light blue lines) can be clearly seen from the time diagram. The thickened vertical lines on the right indicate the prominent presence of penumbrae as well.

4.4 Pulse Rejection, 30Hz Operation

The pulse rejection mode of operation is very similar to that using the double disks as discussed in the last chapter, though phasing the choppers to both limit the neutron bandwidth and eliminate the neutron leakages below 35Å is no long as straight forward as with double-disks. The *maximum* useable neutron bandwidth without having leakages from the rejected pulse is again ~ 4.6Å, regardless where the detector is located between 15-25m. At the shorter distance of 15m, the difficulties of eliminating shorter wavelength leakages from the rejected pulse make it practically useless for pulse rejection.

Table 14 shows the chopper phases that will stop all leakages below 35Å from both the chosen and the rejected pulse for the instrument operating in at the detector distance of 25m in the second frame. Neutron band pass plots from the chosen and rejected pulses are also shown.

Table 14. Chopper phases for 30Hz operation at the detector distance of 25m in the second frame. The chopper openings are as shown in Table 8. As for the case of double-disk choppers, the maximum useable neutron bandwidth without leakages from the chosen and rejected pulses is ~4.6Å.

Frame No.	Chopper	Location [m]	Open At [ms]	Open Duration [ms]	Open Angel [°]	Frame Width [Å]	Umbra [Å]
2-3	T1	5.7	4.8116	11.2585	121.5922	3.303-7.912	3.339-7.846
	T2	7.8	5.2433	15.2930	165.1645		
	T3	9.5	0.4410	18.5590	200.4373		

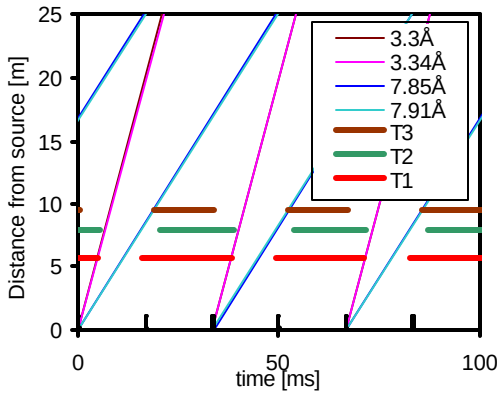

Figure 25. Time diagram with pulse rejection in the second frame for the detector distance of 25m. See Figure 5 for explanation. The chopper openings are as shown in Table 8 and the chopper phases are as listed in Table 14. The phase shifts of the choppers are visible in the diagram

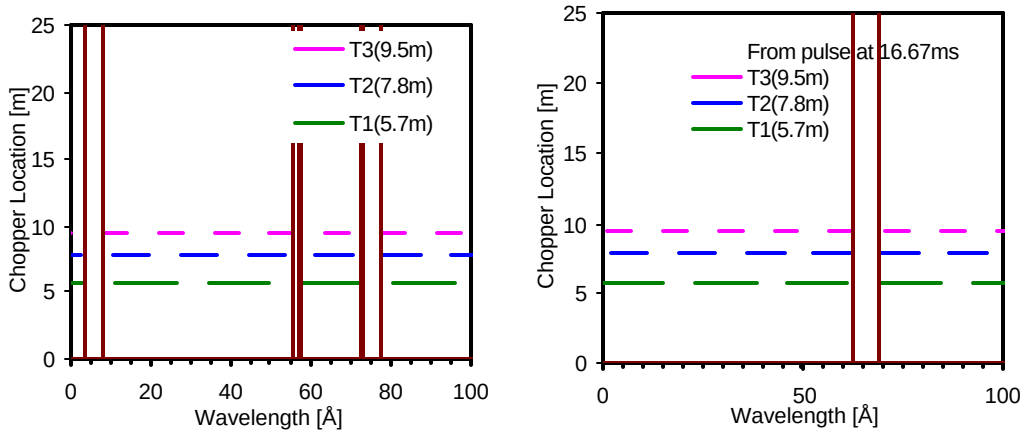

Figure 26. Band pass through the bandwidth choppers in the second frame for the detector-to-moderator distance of 25m. See Figure 6 for explanation. Left: from the chosen pulse. Right: from the rejected pulse. The chopper openings are as shown in Table 8 and the chopper phases are as listed in Table 14. An initial neutron pulse width of 20 ms/Å is used for the calculation of neutron leakages.

4.4.3 Two-Pulse Rejection

Similar to discussions with double-disk choppers, operation with two-pulse rejection will not be feasible on the EQ-SANS.

4.5 Monte-Carlo Verification

Monte Carlo Verification of neutron transmissions through the chopper system is carried out with the chopper design parameters as listed in Table 1. The setup for the simulation is shown in Figure 27.

Figure 28 shows the neutron counts on the detector at 18m. The leakage around 40Å is about 3 orders of magnitude lower than the selected neutron band due to the reduced source flux at that wavelength region.

Figure 29 shows the comparison between the Monte Carlo simulation and the analytical leakage plot. The discrepancies seen for long wavelength neutrons (~75Å) are most likely dues to the fact the gravities are taken into account in the Monte Carlo simulation only.

Figure 30 shows the data around the selected neutron band. Leakages of short wavelength neutrons due to reduced chopper neutron absorptions can be seen. A shoulder-like feature on the left side of the neutron band is also seen due to the fact that the choppers are phased to block neutrons delayed up to 100μs/Å after the initial source pulse only.

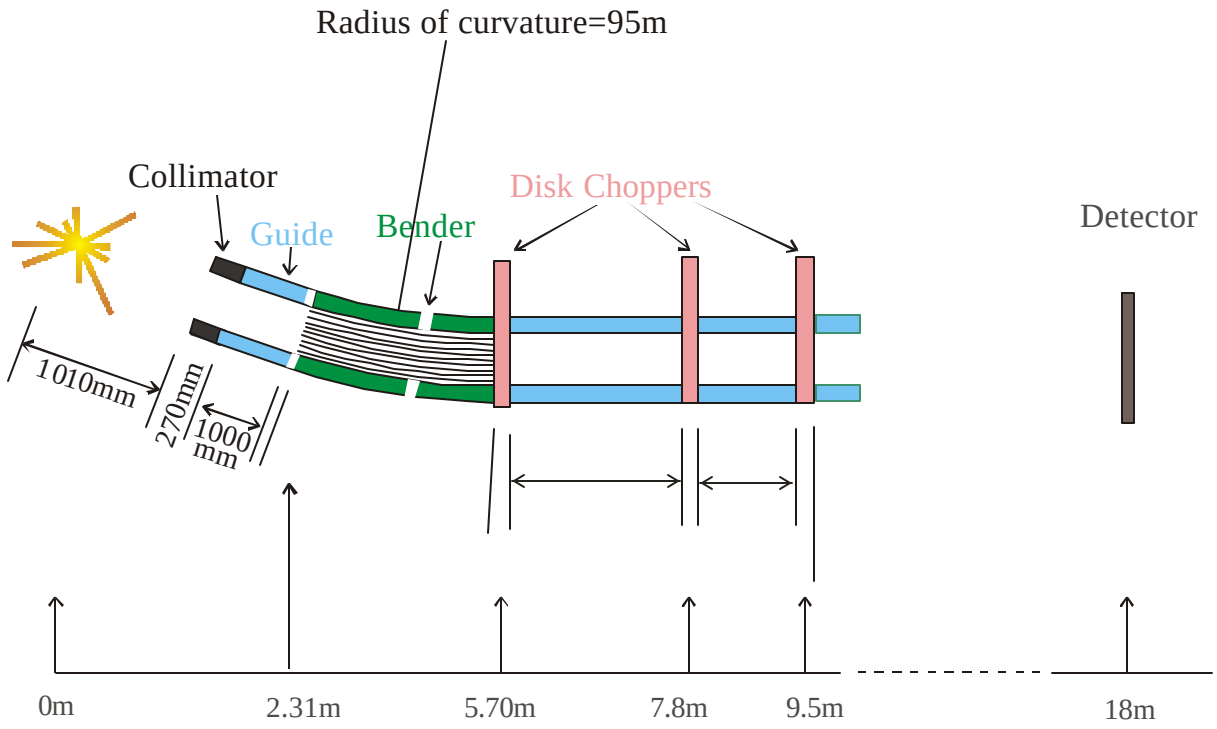

Figure 27. Schematic setup for the M.C. simulation. The chopper window openings are as listed in Table 1. The neutron optics is set as the following. A 270mm long collimator starts 1.1m from the moderator, followed by a 1m-long straight guide. The Bender has 6channels, is 3.3m long, and has the bending radius of 95m. Straight guides follow the bender up to the location of 10m from the moderator, interrupted by the choppers. The beam cross section is 4cmx4cm. The supermirror coatings for all guides and benders is $3.5xq_{Ni}$. The detector is located at 18m. The choppers are phased for the second frame at 18m and are adjusted to block delayed neutrons up to 100ms/Å. The Chopper phase delays are: 5673.5ms, 7698.9ms, and 9338.5ms for T1, T2 and T3, respectively. The transmission for the chopper disks are set to 10^{-7} for 1Å neutrons.

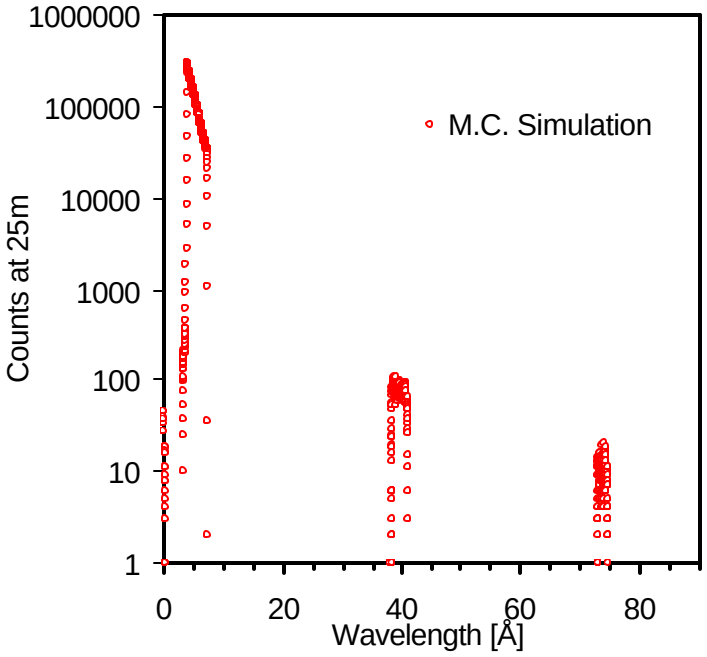

Figure 28. Neutrons that pass the chopper system and arrive at the detector at 18m.

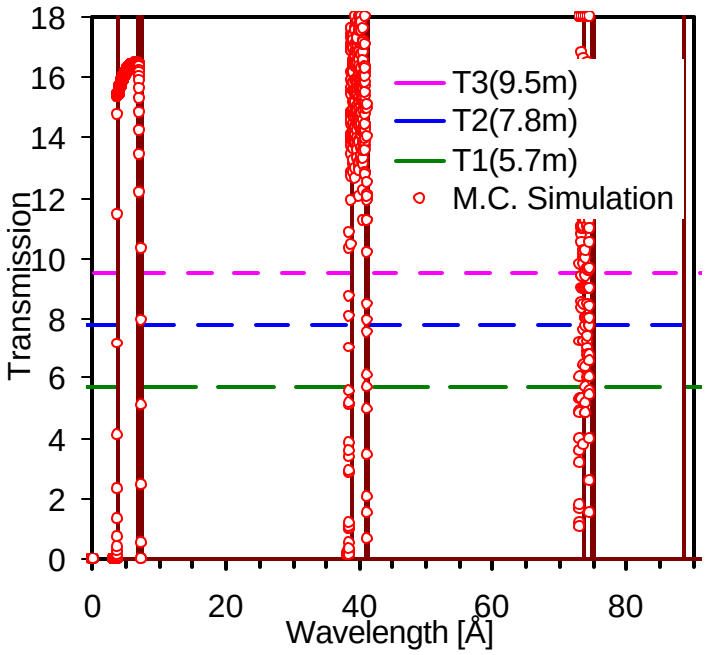

Figure 29. Neutron transmission through the chopper system simulated using Monte Carlo program *IB* (circles) and by analytical methods (vertical solid lines). The Monte Carlo simulation data are taken from Figure 28 and normalized by the monitor counts measured at the entrance of the optical system, namely at 1.1m from the moderator (Figure 27). A scaling factor of 18 is multiplied to the simulation data after the normalization.

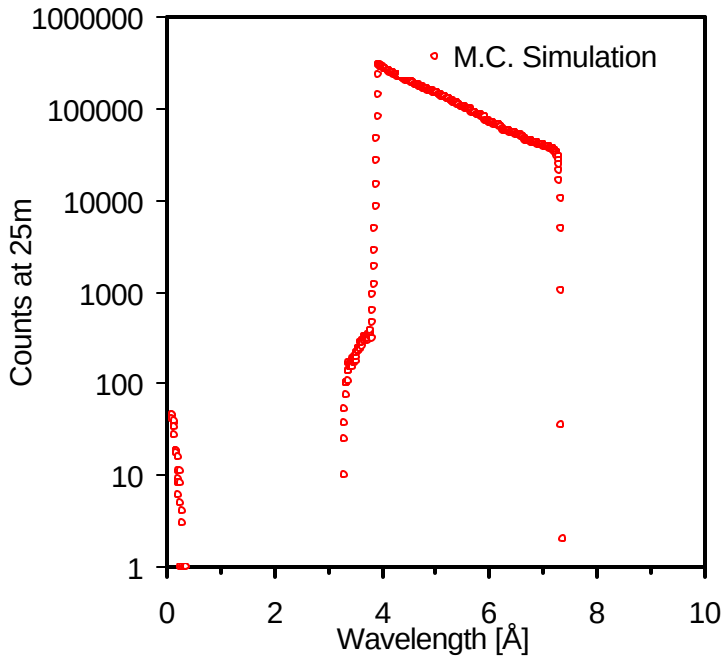

Figure 30. Data from Figure 28 plotted up to 10 Å only. Neutrons with very short wavelength pass through the chopper system because of the reduced absorption by the chopper disks. The shoulder-like feature on the left edge of the selected neutron band is due to the fact the choppers are phased to block neutrons that are delayed up to 100ms/Å after the initial source pulse. Shorter wavelength neutrons that are delayer even longer pass through the chopper system and show up in the shoulder area of the plot.

5. One double-disk, two single-disk choppers

With one double-disk and two single-disk choppers, the chopper system can cover most of the functions as provided by three double-disk choppers. Since the T_1 chopper is located the closest to the moderator, having the T_1 as double-disks should provide the most effective blockage for frame overlaps and leakages. However, T_3 chopper is located closer to the sample area and will be easy to access, upgrading the T_3 chopper to double-disks in the future would be an easier task. Hence, in this chapter, we consider the T_1 and T_2 choppers as single-disk and the T_3 chopper as double-disk.

With the T_3 chopper having variable openings, the single-disk choppers T_1 and T_2 can now have wider openings to allow maximum neutron bandwidth at the shortest detector distance of 15m on the EQ-SANS. The test would then be whether the chopper system will properly function for the maximum detector distance of 25m, which turns out to be the case.

In the following table, the chopper phases as well as the opening for the T_3 chopper are shown for the instrument operating at the detector distance of 25m in the second frame. With the T_1 and T_2 choppers have the widest openings that will ever be needed on this instrument, namely those as determined by the frame width at the detector distance of 15m, no leakage is seen in the second frame at 25m (Figure 31).

Table 15. Chopper phases and opening time intervals for the detector distance of 25m in the second frame. The openings for T_1 and T_2 are fixed as determined by the frame width at the detector distance of 15m and with the initial neutron pulse width ignored. The opening for the T_3 chopper varies dynamically.

Frame No.	Chopper	Location [m]	Open At [ms]	Open Duration [ms]	Open Angel [°]	Frame Width [Å]	Umbra [Å]
2	T1	5.7	3.8316	6.3333	136.8000	2.637-5.283	2.659-5.239
	T2	7.8	5.2433	8.6667	187.2000		
	T3	9.5	6.3861	6.3006	136.0936		

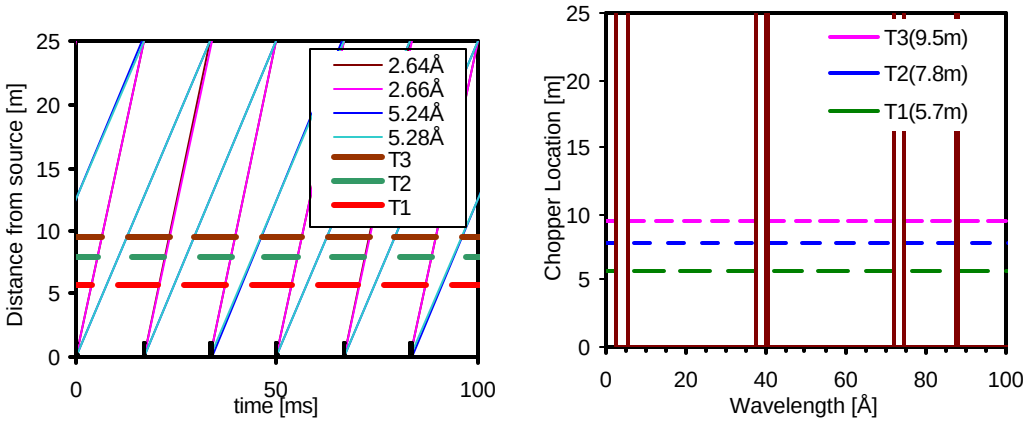

Figure 31. Time diagram and neutron band pass through the bandwidth choppers in the second frame for the detector to moderator distance of 25m. The chopper phases and opening window sizes are as shown in Table 15. A pulse width of 20 ms/Å was used in the time diagram and leakage calculations.

6. Higher Speed Choppers

For future upgrades, high-speed choppers are foreseen for the EQ-SANS to separate elastic and inelastic scattering contributions [ref 2]. In this regard, double-disk chopper have the advantage of having the ability of counter rotation for increased resolution (figure 32). It also provides a way for dynamically varying the chopper windows size since in this inelastic mode of operation, the sizes chopper windows are on the order of the neutron beam cross section (~ 4cm), which is much smaller than that needed for the frame elimination operations in SANS mode.

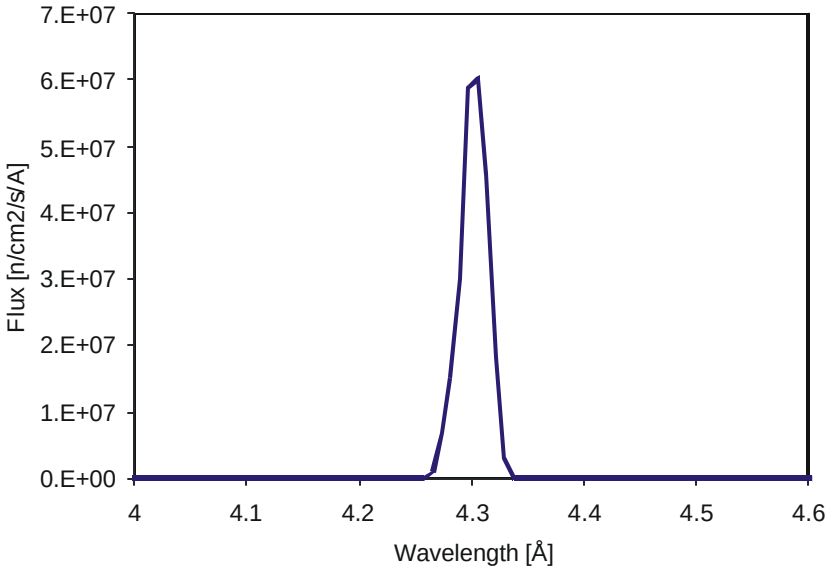

Figure 32. A Monte Carlo simulation from reference [2] of an incident pulse measured on the detector at 18m with 300Hz counter rotating chopper disks. The neutron pulse corresponds to an energy of E_i ~ 4.4 meV and have a dE_i/E_i (FWHM) of ~ 1.2%.

7. Long Wavelength Neutron Reflector

Up to now, we have used the 35Å as the upper wavelength boundary for testing neutron leakages. Neutrons with wavelength longer than 35Å will be removed from the incident neutron beam by a beam reflector. The reflector will be either natural nickel or ^{58}Ni coated silicon or glasses.

Figure 33 show the schematic of a nature Ni coated reflector. The maximum neutron beam divergence that the EQ-SANS is designed to use is nominally ±1°. Within this divergence range, the shown reflector will remove all neutrons with wavelength longer than 35Å. Neutrons with wavelength between 15-35Å are partially removed depending on their wavelengths and divergences. From discussions in previous chapters, the only operation mode where 15Å neutrons are used is in the fourth frame at shorter detector distances, such as 15m (chapter 3). However, fourth frame operations at shorter distances are very unlikely. Therefore, partially removing the 15Å neutrons should not affect the performance of this instrument.

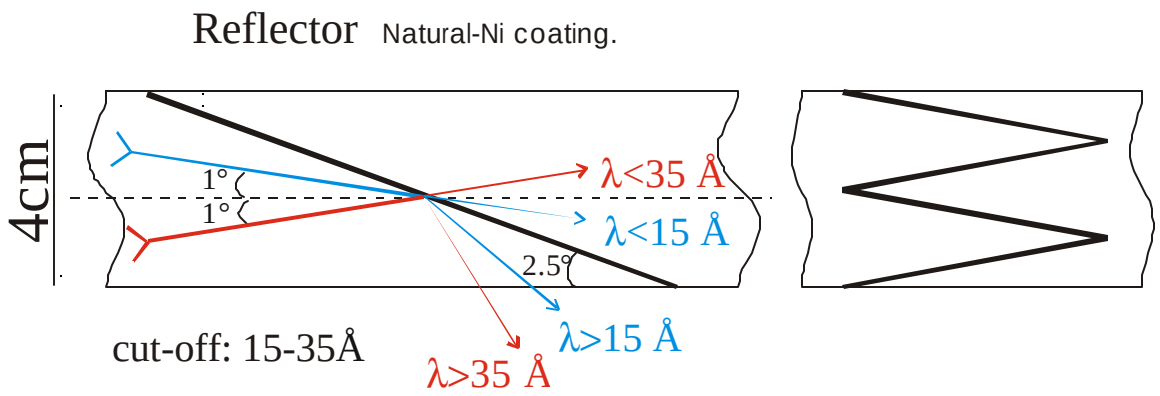

Figure 33. Left: schematic of a long wavelength neutron reflector. A 92 cm long, nature Ni-coated thin glass or silicon is placed in the neutron beam at a 2.5 °angle. Within the divergence of ±1° for the incident beam, all neutrons with wavelength longer than 35 Å will be reflected out of the beam. Neutrons with wavelengths between 15Å-35Å will be partially removed, depending on their wavelengths and divergences. Right: An alternative layout for the beam reflector, made of four pieces of shorter Ni-coated glasses.

References

1. Conceptual Design and Performance Analysis of the Extended Q-range, High Intensity, High Precision Small Angle Diffractometer for SNS, May 2000, Jinkui Zhao, SNS report No. IS-1.1.8.2-6036-RE-A-00 and SNS 107080100-TD0001-R00
2. Supplement to the Extended Q-range, High Intensity, High Precision Small Angle Diffractometer. SNS 107080100-TD0002-R00
3. Optical Components for the Extended Q-Range Small Angle Diffractometer at the SNS. SNS 107080600-TD0001-R00